Regular Article

ANALYTICAL
AND BIOANALYTICAL
CHEMISTRY
RESEARCH

Published by the
Iranian Chemical Society

***Anal. Bioanal. Chem. Res.**, Vol. 10, No. 2, 205-225, April 2023.*

Improving Electrochemical Performance of Polypyrrole Coating by Graphene Oxide-Carbon Nanotube and Zinc Oxide Nanorods in the Role of a Sensor for the Simultaneous Measurement of Morphine and Methadone

Zahra Nazari[a], Zarrin Es'haghi[a,*] and Hongyang Liu[b]

[a]*Department of Chemistry, Payame Noor University, 19395-4697, Tehran, Iran*

[b]*Shenyang National Lab for Materials Science, Institute of Metal Research, Chinese Academy of Sciences, China*

(Received 27 September 2022, Accepted 3 December 2022)

The current research examines the designation of an electrochemical sensor for the simultaneous measurement of morphine and methadone using graphene oxide/multi-walled carbon nanotube/zinc oxide nanorods/polypyrrole nanocomposite, coated on the surface of the graphite electrode reinforced by a hollow-fiber. Its performance was investigated by voltammetry methods while the nanocomposite structure was confirmed by FTIR, EDX, XRD, and SEM techniques. To optimize the effectual factors, the Taguchi test designing method with L_{27}(3x7) orthogonal array was applied. The voltammetric analysis showed that two irreversible oxidation peaks appeared at the potentials of 0.81 V and 0.41 V for methadone and morphine, respectively. Furthermore, the electrochemical investigations showed that the oxidation process of morphine and methadone was under the control of the diffusion phenomenon and two electrons and two protons had been exchanged on the surface of the electrode for both analytes. Chronoamperometry was used to measure the diffusion coefficient soft drugs which were found for morphine and methadone to be 5.31×10^{-6} cm^2 s^{-1} and 1.19×10^{-6} cm^2 s^{-1}. Under optimal conditions, for morphine, two linear concentration ranges of 0.04-10 µM and 10.0-100 µM and a detection limit of 0.01 µM were noted whereas for methadone, two linear ranges were observed in 0.06-8.0 µM and 8.0-100 µM and the detection limit was0.02 µM. The designed sensor can be well used for the simultaneous measurement of the drugs with relative recovery percentages in the range of 98.80-100.22% for morphine and the range of 98.14-100.58% for methadone.

Keywords: Narcotic drugs, RGO-MWCNT with ZnO in PPy, Electrochemistry sensor, Biological samples

INTRODUCTION

Morphine (Fig. AS1) under the IUPAC name of (5alpha,6beta)-7,8-didehydro-4,5-epoxy-17-methyl-morphinan-3,6-diol, and Methadone (Fig. BS1), under the IUPAC name of (Rs-6-(dimethylamino)-4,4-diphenylheptan-3-one) are known as narcotic drugs belonging to the opioid family [1,2]. Morphine is naturally found in the papaver somniferum (the opium poppy), but methadone is synthetically produced.

Methadone and morphine affect the central nervous system as well astheopioidreceptors and although having analgesic, sedative, and detoxifying effects, theycausestrongphysical and psychological dependence [3]. Methadone is normally used to treat drug abuse. As it has a less addictive effect, it is in practice used for quitting drugs such as morphine. The lifespan of methadone is longer than that of morphine because it remains in the liver and other tissues due to its lipophilicity and does not disperse quickly [4].

Today, teenagers and young adults are more on drugs due to economic, social, and psychological pressures, and consequently, death due to drug abuse, especially morphine, has increased [5]. The simultaneous use of these narcotics

*Corresponding author. E-mail: zeshaghi@pnu.ac.ir

with other medications may cause major drug interactions and lead to a breakdown of the central nervous system. Therefore, in order to prevent fatality from drug intoxication in patients, a speedy diagnosis and monitoring of the concentration of morphine are vital, so, the accurate measurement of the amount of methadone and/or morphine in the blood and urine becomes all the more essential. Investigation and measurement of narcotics in biological fluids are also carried out in the fields of forensic medicine and pharmaceutical studies, *etc*.

Today, numerous methods exist to measure the amount of morphine and methadone in substances, such as high-performance liquid chromatography [6], high-performance liquid chromatography-mass spectrometry [7], optical methods such as spectrophotometry [8-9], chemiluminescence [10-11], mass spectrometry [12] as well as electro chemical methods [13]. Among the various techniques mentioned above, chromatography is a typical method, but due to its relatively high cost and long analysis time, as well as the need for highly pure materials and user skill, and in some cases, low sensitivity, it is sometimes disregarded. Instead, electrochemical techniques have received much attention due to their high selectivity, simplicity, high speed, high sensitivity, low detection limit, and reasonable price. The availability of an array of electrodes has also added to this popularity [14].

However, some limitations such as interference with other varieties in real samples, the contamination of the electrode surface, and/or slow electron transfer have made electrochemists modify electrodes in the last decade [15,16]. Due to their increased sensitivity, efficiency, and suitable selectivity, an assortment of surface-modified electrodes is widely used these days for the quantitative determination of a variety of elements.

Electrode surfaces are modified with different nanomaterials in order to facilitate electron transfer and to eliminate limitations such as interference with other varieties in real samples as well as to increase sensitivity and selectivity, and lower detection limits. Many researchers opt for conducting nanomaterials to modify electrode surfaces, for instance, the sensitivity of sensors can be improved by forming graphene nanocomposite carbon nanotubes (CNT). Multi-walled carbon nanotubes include a number of concentric tubes in a regular structure. With a high ratio of length to the radius, they have features such as low weight, high strength, permeability, electrical conductivity, high stability, and high specific surface area (from tens to a thousand square meters per gram), all of which increase the speed of low electrochemical reactions and facilitate electron transfer.

Graphene is a two-dimensional gapless semiconductor that is capable of providing a large surface area suitable for performing electrochemical reactions with optimal conductivity through its unique mechanical, electrical, and optical properties [17]. Among graphene and its derivatives, reduced graphene oxide (RGO) has become popular for modifying the surface of electrodes which is due to an electrical conductivity 8 times higher than that of graphene oxide [18].

Furthermore, zinc oxide (ZnO) is another one that has attracted wide attention due to its unique properties such as a wide band gap, the high exciton binding energy (approximately 60 millivolts), high mobility of conduction electrons, physical and chemical stability, electrical conductivity, high catalytic activity, low toxicity, increased band gap, an increase in electrical properties, and the high surface-to-volume ratio [19]. In fact, it has been widely used to make various kinds of sensors, especially gas sensors [20]. Polypyrrole (PPy) has high conductivity, appropriate environmental stability, sensitivity, and selectivity [21]. Moreover, alinkwith ZnO semiconductor nanoparticles which have good electron acceptance and high sensitivity cause a synergistic effect by amplifying the characteristics and can be used in the production of all kinds of sensors [22]. As mentioned above, the synergy of CNT, ZnO and PPy composites improve sensitivity and conductivity.

The present research is focused on the fabrication of a nanocomposite-based modified sensor, RGO-MWCNT with ZnO in PPy. The improved composite enhanced the electrical conductivity and the sensitivity of the new electrochemical sensor which became the working electrode for the simultaneous determination of morphine and methadone.

A preparation technique such as microextraction is commonly used for sample preconcentration and drug separation. Among these, SPME or Solid Phase Microextraction is one of the most appealing methods, but the number of coatings that can be used in it is limited, and molecules with a high molecular weight may be absorbed on

the surface of the fiber, so there might be a residual effect of the previous test on the subsequent one [23]. Thus, in some cases these days, a modifying method called solid/liquid phase microextraction based on modified hollow fiber is preferred; this was first introduced by Es'haghi *et al*. [24].

The hollow fiber in this system would play the role of a solid/liquid microextraction device and simultaneously, serve as the homemade hollow fiber graphite working electrode for the determination of the drugs. Our idea was based on the use of a polypropylene hollow fiber membrane that operates as an analyte trap, among the acceptor solvent in the lumen and pores of the hollow fiber. This system caused higher selectivity and enrichment because the solvent accumulated in the lumen of hollow fiber preconcentrates the analyte prior to the electrochemical process.

In the current study, we placed nanoparticles in the polypropylene hollow fiber through quaternary salts, as per the SPME device. Quaternary salts consist of one cation and one anion; the former includes bulky organic groups such as imidazolium, pyridinium, pyrrolidine, ammonium, and phosphonium, and the latter includes organic anions such as trifluoromethyl sulfonate, and trifluoroacetate, or mineral anions such as chloride, bromide, nitrate, perchlorate, tetrafluoroborate, and hexafluorophosphate [25].

Due to their high electrical conductivity, Quaternary salts- like ionic liquids-improve the electrocatalytic properties of carbon nanoparticles and the stability of various modifiers, including electrode modifiers. Therefore, the resulting membrane activated by nanoparticles acts as an analyte trap with higher factor enrichment and selectivity. So, it is necessary to bind the analyte by both covalent and non-covalent chemical methods. As the results show, there is a considerable improvement compared to the conventional hollow fiber SPME method [24]. In this work, the hollow fiber used in solid/liquid phase microextraction was coupled with an electrochemical system.

The disposable nature of the electrode protected with hollow fiber reduces the interference of previous experiments, and its easy preparation process, low background current, high sensitivity and stability, and the usage of nanoparticles in this method create possible and practical potentials for making new sensors for important varieties.

The effect of some major parameters on the efficiency of the method and the determination of optimal laboratory conditions for the simultaneous measurement of two analytes were taken into account and the test was designed *via* the Taguchi method to optimize the chemical process, all of these factors led to a systematic approach being obtained whose benefits included cost and time reduction, simpler design and a more efficient method for extracting and measuring target analytes [26].

Although there are a large number of studies on the separate (individual) measurement of methadone and morphine, library data show that the simultaneous measurement of these compounds using modified electrodes has not been reported yet. Moreover, because methadone is used to help morphine and heroin (opioid) addicts gain their health, the timely measurement of methadone and morphine in the blood can show the amount of the same in their bodies and the progress of their recovery process.

Given the advantages of electrochemical, electrode surface modification, and experimental design methods, the main goal of this study was to build an electrochemical sensor using a modified electrode with adequate selectivity and high sensitivity which would be appropriate for the simultaneous detection of methadone and morphine in the matrix of real biological samples.

EXPERIMENTAL

Reagents and Chemicals

The chemicals, ethanol, graphite, potassium permanganate, pyrrole, zinc sulfate ($ZnSO_4 \cdot 7H_2O$), sodium hydroxide, sodium chloride, disodium hydrogen phosphate, iron(III) chloride, sodium dihydrogen phosphate, ethanol hydrogen peroxide, acetone, cetyltrimethylammonium bromide (CTAB), hydrochloric acid, phosphoric acid, ferric chloride ($FeCl_3 \cdot 6H_2O$), potassium hydroxide, acetonitrile and N,N-dimethylformamide of analytical purity degree were all obtained from the German company, Merck, and used without purification.

Morphine sulfate and methadone were obtained with a high degree of purity (<99%) from DarouPakhsh Co. (Tehran, Iran). Double-distilled water (ddH_2O) was used in all experiments, and the electrical conductivity of ultrapure water was 5.15×10^{-6} MΩ CM [27]. Multi-walled carbon nanotubes with a purity degree higher than 95%, a density of

2.1 g cm^{-3}, a specific surface area of 110 m^2 g^{-1}, an inner diameter of 5-10 nm, an outer diameter of 20-30 nm, a length of 10-30 microns and electrical conductivity above 100 S/cm, and synthesized via the chemical vapor deposition approach (CVD) were obtained from American US Research Co.

The hollow fiber polypropylene membrane support Q3/2 Accurel PP (200 μm thick wall, 600 μm inner diameters, and 0.2 μm average pore size) was purchased from Membrana (Wuppertal,

Germany). The hollow fiber was cut into 2 cm pieces. Next, the fibers were placed in acetone to be cleaned and ready for use.

A solution of 0.1 M potassium chloride and one-millimolar $[Fe(CN)6]^{-3}$/$[Fe(CN)6]^{-4}$ solution was used as the electrochemical probe to determine the effective cross-section of the modified electrode.

The phosphate buffer solution was prepared by adding dilute solutions of H_3PO_4, KH_2PO_4, and KOH 0.1 M, and, the acetate buffer was made by adding dilute KOH solution to 0.1 M acetic acid solution and then the pH of the resulting solutions was adjusted using a pH-meter device.

Equipment

The electrochemical experiments were conducted in this research using a potentiostat/galvanostat device model BHP 2066 made by Behpazhooh Company (Tehran, Iran) with three electrodes, namely, Ag/AgCl/KCl 3 M electrodes as reference electrode, platinum wire as the auxiliary electrode, and a graphite electrode modified by core/shell quantum dot (CdSe) ZnS, withmulti-walled carbon nanotubes as working electrodes. As the graphite electrode, a pencil graphite (2B, the diameter of the pencil is 0.5 mm and a length of 8 cm) has been used. The samples prepared from this sensor underwent characterization. Before recording the XRD patterns, the electrode was dried. EDX analysis was performed using an Energy Dispersive X-ray Spectroscopy with a silicon detector and the FT-IR device was used to record the IR spectrum.

X-ray diffraction analyses were carried out using Siemens D500 (Germany). The (Czech) Tescan scanning electron microscope (SEM) was used to determine the surface morphology, while an infrared spectrometer (FT-IR, Bruker Tensor 12 made in Germany) was used to record the IR spectrum. A German-manufactured scanning electron microscope (SEM), Zeiss, was utilized to determine the surface morphology. A German-made ultrasonic processor UTR200 was used for the synthesis of cadmium selenide, while the pH of the solutions was adjusted using a PHS-550 laboratory pH meter made in Switzerland.

Synthesis of RGO-MWCNT-ZnO/PPy Nanocomposite

Graphene oxide. The synthesis of graphene oxide was carried out according to Hummers Method with slight modifications such that, 2 g of graphite powder was added to 45 ml of concentrated sulfuric acid and stirred at a medium speed for 2 h. Then, while the container was placed in a cold-water bath, the temperature was controlled at 20 °C, and 6 g of potassium permanganate was carefully added to it. The materials were stirred for 2 h at a temperature of 35 °C. Next, the container was immersed in an ice-water bath, and 100 ml of deionized water was added while being stirred. Then, the solution was heated and kept at 90 °C for 30 min. After that, 10 ml of 30% oxygenated water and another 150 ml of deionized water were added to the previous materials. The resulting graphite oxide suspension was placed in a stationary state so that the graphite oxide settled and the upper liquid overflowed. In the next step, 20 ml of 5% hydrochloric acid aqueous solution was added. The mixture was thoroughly stirred and after the solution settled, the overflow liquid was removed. Then about 100 ml of deionized water was added and the mixture was stirred again and settled. After the material settled, water was poured over it until the acidic state of the solution changed and the solution reached neutral pH. 160 ml of deionized water was added to the resulting graphite oxide precipitate, and it was stirred under ultrasonic waves for 1 h until the graphite layers were separated and single layers of graphene oxide were obtained. After centrifugation, the sediments were separated and dried at 60 °C [28].

Oxidation of carbon nanotubes. In order to purify carbon nanotubes to remove catalytic impurities and amorphous carbon, they were first heated at 400 °C for 40 min. In the next step, in order to oxidize the purified nanotubes, the first 10 ml of nitric acid and 30 ml of concentrated sulfuric acid were mixed in a ratio of 3:1 and brought to a volume of 40 ml. Then, 0.5 g of carbon nanotubes were added to the solution. The mixture was placed on a hot plate and refluxed at 80 °C for 8 h.

After the oxidation of the nanotubes, carboxyl, hydroxyl, and carbonyl functional groups were placed on the surface and inside the layers of nanotubes, and this increased the porosity and activated the multi-walled carbon nanotubes. The specific surface area of nanotubes increased and their adsorption capacity for materials increased. In order to remove excess acid, the carbon nanotubes were washed in several steps with a sufficient amount of deionized water until the pH reached about 7. Then, the active nanotubes were dried in the oven for 4 hours at 70°C and kept in a desiccator [30].

Synthesis of ZnO nanorods. To synthesize ZnO nanorods, two precursors, zinc sulfate ($ZnSO_4 \cdot 7H_2O$) and sodium hydroxide were separately dissolved in double distilled water to obtain a molar ratio of 1:3. For this purpose, 1.438 g of zinc sulfate ($ZnSO_4 \cdot 7H_2O$) was placed in a 50 ml volumetric flask and distilled water was added until it dissolved. And in another 10 ml volumetric flask, 0.816 g of sodium hydroxide was put and distilled water was added. Then, 3 g of CTBA was poured into a 250 ml beaker and 50 ml of distilled water was added to it and the temperature was brought to 80 °C. Then, 7 ml of prepared sodium hydroxide solution was added to it and 50 ml $ZnSO_4 \cdot$ Next, $7H_2O$ solution was added drop by drop to the mixture of NaOH and CTAB, while it was being vigorously stirred on an electric heating stirrer, and the mixture was kept at 80 °C temperature for 5 h. The obtained white precipitate was separated by centrifugation and washed with distilled water several times and dried at 70 °C in an oven for 2 h. Finally, the resulting product was calcined at 200 °C for 3 h [31].

Preparation of RGO-MWCNT composite. In a 100 ml beaker, 100 mg of graphene oxide was poured into 50 ml of distilled water and sonicated for 30 min. In another 100 ml beaker, 100 mg of multi-walled carbon nanotubes were poured into 50 ml of distilled water and sonicated for 30 min. Then, the multi-walled carbon nanotubes were transferred to a balloon and the graphene oxide solution was continuously poured drop by drop and stirred at room temperature for 24 h.

In the next step, 1 mole of hydrazine hydrate (6.03 ml) was added to the flask and the temperature was increased to 100 °C, and the reflux process was performed for 24 h at this temperature. Multi-walled carbon nanotubes were absorbed on the GO surfaces due to strong π-π interaction. In the next step, the solution was cooled and the GO/MWNT was separated by nanocomposite centrifugation, and the resulting precipitate was washed several times with distilled water [32].

Preparation of RGO-MWCNT-ZnO nanocomposite based on polypyrrole. The weighted amount of 1:1 of the mixture (RGO-MWCNT-ZnO) was poured into 50 ml of aqueous solution (0.7 g of iron(III) chloride, $FeCl_3$) and homogenized by stirring with ultrasonic waves for 30 min. Then 2 ml of pyrrole was added dropwise under continuous and vigorous stirring, and the mixture was placed on the stirrer for 3 h. The nanocomposites were filtered and washed several times with distilled water and then dried at 60 °C [33].

Preparing and Modifying the Electrode Surface

Preliminary stage of electrode preparation. Before modifying the surface of the graphite electrode with RGO-MWCNT-ZnO/PPy nanocomposite first, the electrode was washed several times each time with double distilled water. Then, the bare electrode was placed in acetone for 10 min to remove any organic contamination. Finally, it was washed several times with double distilled water. After completing the above operation, the graphite rods were dried at room temperature for 24 h.

Modification of the electrode surface. To deposit the synthesized nanocomposite on graphite, a certain amount of the nanocompositeRGO-MWCNT-ZnO/PPy (according to the Taguchi procedure) was added to 10 ml of N,N-dimethylformamide (DMF) and subjected to ultrasonic waves for 15 min. Then, the graphite rods that had been prepared in the previous step were immersed in this mixture. After immersion in ambient temperature (three times and 4 h each time), they were dried.

In the second step, the polypropylene hollow fiber was cut into 2 cm pieces. The parts were washed with acetone to remove impurities, and after several times of washing with distilled water, they were dried in the open air.1.7 cm of pencil graphite rod modified by RGO-MWCNT-ZnO/PPy nanocomposite was carefully placed inside each piece of the hollow fiber. The free end of the hollow fiber was closed with heat.

Specific ratios of ionic liquid and octanol (50:50 ratio; in a fixed volume of 5 ml) were poured into a 10 ml beaker and a specific amount of modified nanocomposite (according to

Taguchi's table) was added to this solution. The resulting mixture was dispersed under ultrasonic waves for 15 min. Then, the hollow fiber was placed inside the mixture of solvent and nanoparticles, and it was stirred by ultrasonic waves for 2 min to ensure the transfer of the mixture into the pores of the fiber. After that, the hollow fiber was taken out of the mixture and its outer layer was washed and used as a working electrode.

Preparation of Biological Samples

Samples included blood from 3 healthy volunteers. The serum samples came from a medical diagnostic laboratory and had been prepared from the whole blood samples as per the standard procedures of clinical laboratories.

To prime the samples, the proteins have to be precipitated first, we carried this out by adding 3 ml of acetonitrile to 2 ml of the blood [34] and, then, it was centrifuged for 15 min at a speed of 3500 rpm. For determining the concentration of morphine and methadone using the prepared electrode, the method of standard addition was utilized. In this way, 1 ml of serum (the real sample) was diluted using 10 times the amount of phosphate buffer saline. Then, different amounts of standard morphine and methadone were added to 1 ml of the solution to achieve an array of concentrations (0, 0.2, 0.4, 0.6, 0.8, and 1 μm).

With regards to the urine samples, they were taken from healthy volunteers and centrifuged at 3500 rpm for 10 min. The resulting clear supernatant solution was diluted 10-fold with 7.4 pH saline phosphate buffer and then different amounts of analyte were added to it. In this way, spiked urine samples were obtained with varying concentrations of 0, 0.2, 0.4, 0.6, 0.8, and 1 μm [35].

RESULTS AND DISCUSSION

Characterization of RGO-MWCNT-ZnO/ PPyNanocomposite

To determine the structural characteristics, the synthesized nanocomposites were characterized via scanning electron microscopy (SEM), energy dispersive X-ray (EDX) as well as X-ray diffraction spectrometer (XRD).

Characterization of zinc oxide nanorods. The results of FTIR of oxide nanorods are shown in Fig. S2 (A). The bands formed at 1385 cm^{-1} and 1630 cm^{-1} are attributed to the vibrations of symmetric and asymmetric C=O bonds, respectively. The band at 2364 cm^{-1} corresponds to the vibration of the O=C=O state. The infrared spectrum of zinc oxide (ZnO) usually shows an absorption band between 423 and 507 cm^{-1} due to the stretching vibrations of ZnO, and the broad bands around 3435 cm^{-1} are driven by O-H stretching vibrations on the surface of zinc oxide (ZnO).

In order to investigate the crystal structure and calculate the crystal size of the synthesized nanoparticle, diffraction patterns were prepared from the crystalline powder sample at ambient temperature. In Fig. S2(B), the diffraction peaks at θ 2 = 31.7°, 34.3°, 36.2°, 47.5°, 56.5°, 62.7°, 66.2°, and 68.7° can be seen corresponding to the crystal plates (100), (002), (101), (102), and reflective plates (110), (103), (200) and (112), respectively. All the peaks indexed in the obtained spectrum correspond well to the plates of the hexagonal wurtzite structure of ZnO (079-0207-01) and are consistent with the reference pattern from the Joint Committee on Powder Diffraction Standards (JCPDSNo. 01-079-0207). The average particle size (D) was calculated based on the Debye-Scherrer equation (Eq. (1)):

$$D = \frac{K\lambda}{\beta\cos\theta} \quad (1)$$

where D is the average particle size, λ is the wavelength of x-ray radiation (Kα of copper radiation is equal to λ = 1.54056, β is the peak width at the half height (FWHM), and θ is the Bragg angle (range 2θ is from 5 to 99 degrees).

The crystalline size of zinc oxide nanoparticles (ZnO) was calculated with the FWHM of the mentioned peaks (101), the most intense and longest peak, and from the XRD reflection pattern using Scherrer's equation. The average particle size was found to be 57 nm, based on Scherrer's equation.

In order to investigate the chemical composition of synthesized zinc oxide (ZnO), EDX analysis was undergone, which confirmed the presence of Zn and O (Fig. S2(C)). The elemental analysis of zinc oxide (ZnO) shows that the composition contained 10.24% Zn, 23.53% O, and 40.41% C, which confirmed the formation of pure ZnO. The percentage of carbon observed in EDX is due to the carbon band used for loading the sample in the SEM. The molecular ratio of Zn:O of the cultured nanorods, obtained from EDX

and quantitative analysis data is close to 2:1.

The SEM image of the surface morphology of prepared zinc oxide nanorods is shown in Fig. S2 (E). The size of zinc oxide nanoparticles is in the range of 50-92 nm with a micron diameter, which is almost in accordance with the particle size calculated from the Sherrer formula.

Characterization of graphene oxide. The results of the FTIR of graphene oxide are shown in Fig. S3 (B). The wide peak that appeared in the oxide area of the Graphene showed vibrational bands at 1051 cm^{-1}, 1723 cm^{-1} and 13000 to 3600 cm^{-1}; which is due to the presence of typical oxygen functional groups, C-O-C, C=O, and O-H, respectively. And the observed peak at 1625 cm^{-1} is attributed to the C-C stretching vibration. The surface morphology of graphene oxide in the SEM image in Fig. S3 (C) shows that graphene oxide is layered.

Results from FTIR spectrum of carbon oxide nanotubes. The spectroscopy (FT-IR) of oxidized carbon nanotubes was investigated (S4 A). The symmetric and antisymmetric stretching vibrations of C-H at frequencies of 2825 cm^{-1} and 2854 cm^{-1} and the C=C bond at 1636 cm^{-1} in oxidized nanotubes can be seen. The broad peak is related to the O-H vibrational stretching frequency of 3420 cm^{-1} and the C=O peak at the wave number of 1712 cm^{-1}, which is of the carbonyl group, confirmed the oxidation of nanotubes.

Characterization of RGO-MWCNT. The FTIR analysis of the RGO-MWCNT composite is shown in Fig. S5 (A). The vibrational bond between 2800 and 13000 cm^{-1} belongs to CH_2 asymmetric and CH_3 symmetric stretching vibrations.

The existence of C=C stretching vibration is shown at 11637 cm^{-1}, while the other characteristic peaks, at 3442 and 1052 cm^{-1}, indicate the O-H and C-O groups, respectively. There is a band at 2364 cm^{-1} since there exists a vibration of the O=C=O states. The RGO-MWCNT X-ray diffraction pattern and the diffraction peaks at 2θ values of 25.03° and 43.88° were attributed to the structure of graphite (002) and RGO plate (100) as well as to MWCNTs.

The (002) plate corresponds to the pure hexagonal lattice of RGO. The absence of the characteristic diffraction peak of graphene oxide S5 (B) is the reason for the reduction caused by hydrazine. The FESEMS5 image (C) shows the formation of MWCNT entanglement in the RGO sheet. MWCNT was uniformly distributed and completely wrapped in a sheet. The compound of MWCNT with RGO occurred due to π-π interaction [36].

Characterization of RGO-MWCNT-ZnO/PPy nanocomposite. Conducting polymers (CPs) like polypyrrole plays a noteworthy role to enhance the charge and discharge rates. Polypyrrole is one of the most studied sensor modifiers due to its ease of fabrication and high conductivity when doped. The PPy structure has a significant outcome on the electrical conductivity of sensors Due to the different arrangements created in the PPy chains and the different charge distribution of these models. Also, owing to its porous structure, the PPy-carbon-based modified sensors have a large effective area, so improving the sensitivity of an electrochemical sensor.

The PPy structure involved a conjugated system, with single and double covalent bonds through the overlap of the p orbitals with delocalized electrons (σ- and π-bonds) [21].
In conclusion, the use of metal oxide nanoparticles with carbon-based materials and PPY led to the development of a new category of nanohybrid materials with the integrated properties of all compounds. The adsorption efficiency of RGO-MWCNT-ZnO/PPy nano-hybride was arbitrated in the extraction of analytes.

FT-IR analysis in Fig. 1A confirms the presence of RGO-MWCNT-ZnO/PPy nanocomposite. In the current study, the peak at 1000 cm^{-1} is related to the asymmetric stretching vibration of C-O. The peak at 1500 cm belongs to the vibration of the Amin structure of the second type caused by the stretching vibration of pyrrole. The presence of a peak in the region of 1600-1500 cm^{-1} shows C-C and C-N stretching vibration. In the region of 1600-1800 cm^{-1}, it specifies C=O vibrations. The peak in the region between 2800 and 3000 cm^{-1} belongs to the asymmetric stretching vibrations of CH_2 and symmetric CH_3, and the vibration bond at 3445.94 cm^{-1} shows the N-H and O-H bonds.

Figure 1B confirms the X-ray diffraction pattern of RGO-MWCNT-ZnO/PPy nanocomposite. In this design, the two peaks that appeared at the angles of about 25.88 and 43.58 degrees correspond to the diffraction of the (002) and (100) plates of graphene oxide, respectively. The diffraction peaks at 2θ, 31.7, 34.3, 36.2 47.5, and 62.7 degrees match the crystal plate (100), (002), (101), (102), (110), (103). All the indexed peaks at the current spectrum paired well with the hexagonal wurtzite structure of the ZnOplates (01-079-0207)

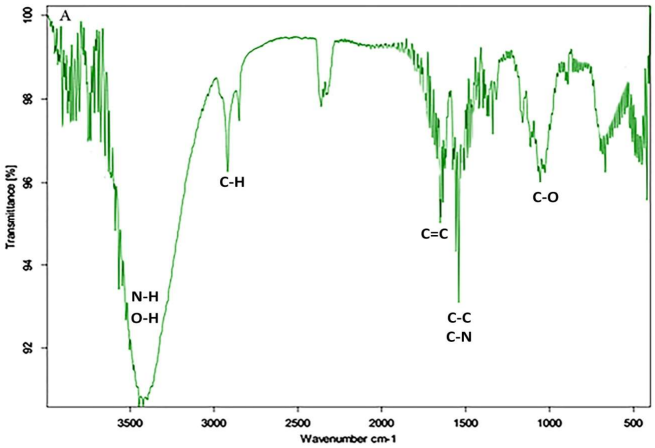

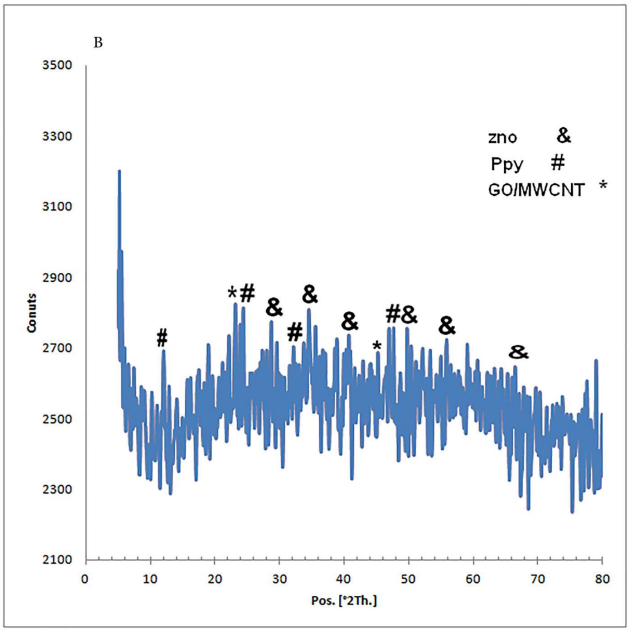

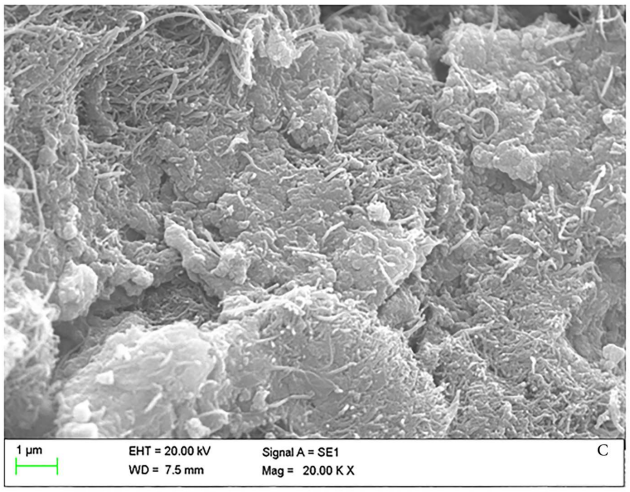

Fig. 1. (A) FT-IR spectra (B) XRD pattern C) SEM images from the surfaces RGO-MWCNT-ZnO-pp powder.

and conform to the reference pattern from the Joint Committee on Powder Diffraction Standards (JCPDS No. 01-079-0207).

Four diffraction peaks exist related to PPy chains at 2θ, 11.7 degrees, 22.7 degrees, 29.8 degrees, and 44.3 degrees, corresponding to the crystal plates, (101), (102), (110), (311). Diffraction peaks at 22.15 degrees indicate the amorphous nature of polypyrrole.

The appearance of peaks related to graphene oxide sheets, along with peaks related to ZnO and polypyrrole crystal sheets in the X-ray diffraction pattern proves that the RGO-MWCNT-ZnO/PPy nanocomposite has been synthesized. As can be seen in the highest intensity of the mentioned peaks, the average particle size (D) was found to be about 98nm, based on the Scherrer equation.SEM images of the morphology of the synthesized nanomaterials in Fig. 1C show a more uniform and dense distribution of their nanocomposites.

Morphology of Electrode Surface Modified with RGO-MWCNT-ZnO/PPy

The scanning electron microscope was used for structural investigation and morphological studies. The surface of PGE coated with RGO-MWCNT-ZnO/PPy nanocomposite was investigated by SEM technique. Figure 2A shows the surface of the unmodified PGE electrode. By adding the RGO-MWCNT-ZnO/PPy nanocomposite to the PGE structure, the surface area increases dramatically (B). In fact, the RGO-MWCNT-ZnO/PPy hybrid nanocomposite provides a more porous structure for PGE. This increases the active surface of the electrode that is in contact with the electrolyte and electroactive species.

EXPERIMENT DESIGN

This design was produced in two stages. In the first stage, before making the RGO-MWCNT-ZnO/PPy nanocomposite, factors such as the amount of CTBA g, GO/MWNT wt%, GO/MW:ZnO wt%, and pyrrole ml were optimized and considered as factor 1 in time. Other factors such as the amount of RGO-MWCNT-ZnO nanocomposite/PPy, immersion time and the number of immersions, the ratio of ionic liquid to ethanol, amount of nanocomposite inside the hollow fiber, pH, and the scanning speed were optimized

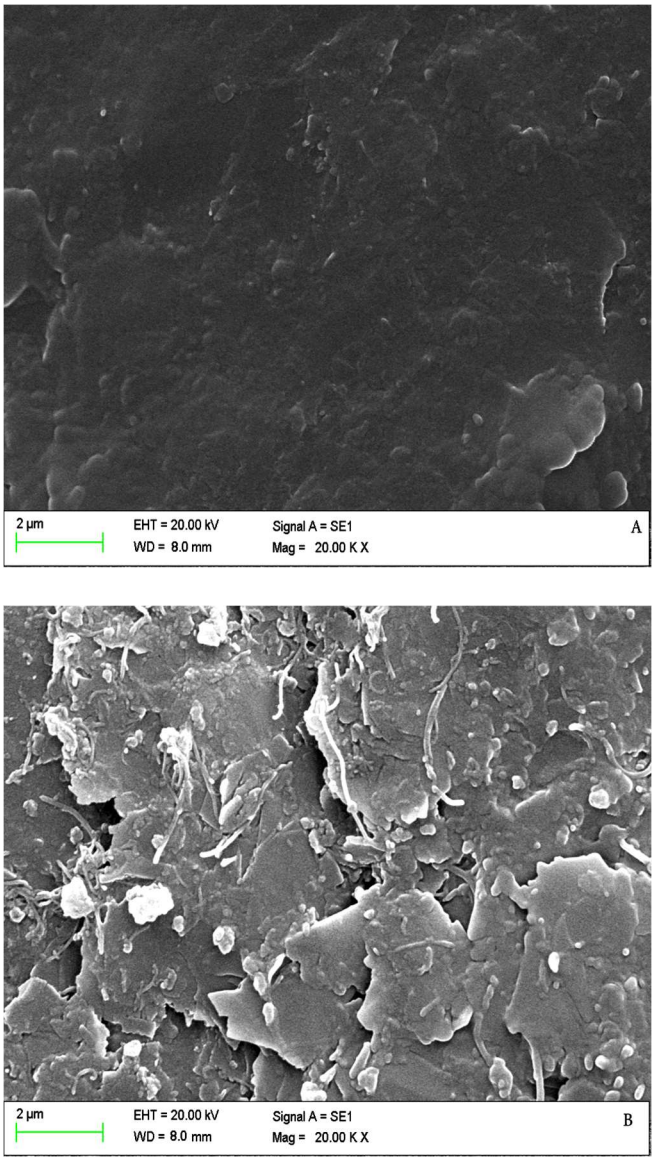

Fig. 2. (A) SEM images of Bare PGE (B). SEM images of RGO-MWCNT-ZnO-pp modified PGE.

with Taguchi software.

Design as a Time Factor

According to Table S1, before preparation, the factors of the RGO-MWCNT-ZnO/PPy nanocomposite, the amount of CTBA g, GO/MWNT wt%, wt% GO/MW: ZnO, and pyrroleml were optimized as one factor in a time. To this end, all the pencil rods were similarly prepared by the immersion method and under the same conditions. The immersion time was 6 hours and an amount of 0.003 g of each substance was placed in 10 ml of N, N-dimethylformamide; and, the measurement was conducted at a concentration of 4 micromolar of morphine and methadone.

According to the observed flow intensity of the two drugs, *i.e.*, morphine and methadone, the optimal values of 3 g of CTBA, GO/MWNT with a weight percentage of 2:1, and GO/MW:ZnO with a weight percentage of 2:1 were determined since the highest amount of flow intensity was found in both the drugs, morphine, and methadone.

Ionic liquids consist of a cation and an anion. The cation usually includes bulky organic groups such as imidazolium, pyridinium, pyrrolidine, ammonium, and phosphonium, and the anion includes either organic anions such as trifluoromethyl sulfonate, trifluoroacetate, or mineral anions such as chloride, bromide, nitrate, perchlorate, tetrafluoroborate, hexafluorophosphate.

Quaternary salts, as a similar and simple type of ionic liquids, improve the electrocatalytic properties of carbon nanoparticles and the stability of various modifiers due to their high electrical conductivity.

In order to investigate the effects of quaternary salts on the performance of this sensor, three types of electrolytes tetraethylammonium chloride (TEAC), tetraphenylphosphonium chloride (TPPC), and tetraethylammonium hydroxide (TEAH) were selected and assessed in terms of any effect on morphine and methadone analytes (concentration of analytes 4 µM); the results of which are reported in Table S2. They indicate that the current response increased after applying the ionic liquid tetraethylammonium hydroxide, therefore this compound was used in the experiments.

Experiment Design with Taguchi Software

The Taguchi technique draws an orthogonal standard representation showing the effect of selected factors on the target values of the experiment. The Taguchi Array has been used for performance evaluation and statistical analysis of the relationships between effective variables, and optimization of the parameters under investigation. Taguchi is a powerful tool for performing minimum tests in the shortest time, reducing costs, and obtaining data in a controlled manner to analyze the effect of parameters influencing the process.

In order to study the factors such as the amount of RGO-

MWCNT-ZnO/PPy nanocomposite in grams (A), the immersion time in hours (B), the number of times of immersion (C), the volume percentage of quaternary salt/octanol (D), the amount of nanocomposite inside the hollow fiber in grams (E), pH (F) and scanning speed in terms of V/S^{-1} (G), they were optimized with Taguchi software by providing an orthogonal L27 (7*3) array. To this end, these seven factors were examined at three separate levels (according to Table S3).

The Mini Tab 16 software was used for the design of the experiment and statistical analysis. The response of the sensor and the S/N value related to this L27 orthogonal presentation are shown in Table S4. In this table, the sum of currents resulting from the oxidation peak of morphine and methadone in a 4-micromolar solution of each of these substances was measured by the differential pulse voltammetry (DPV) technique. In order to increase reproducibility, the analyses were repeated three times under the same conditions and the average responses were calculated for each factor at different levels.

Examining the variables. The average signal-to-noise ratio S/N for each level of electrode response factor is shown in Fig. 3. The highest value of signal-to-noise determines the optimal level of that factor. Therefore, the optimal amount of nanocomposite RGO-MWCNT-ZnO/PPy is equal to 0.006 g, the duration of immersion is 4 hours, the number of immersions is 3 times, and the scanning speed is 0.1 V/S^{-1}.

The solvent ratio of octanol-quaternary salt (0-100), that is 100% of quaternary salt, was chosen as the optimal factor. Moreover, the amount of nanocomposite inside the hollow fiber is 0.00 with a pH of 7.4. Since the greater the slope of the signal-to-noise graph is, the greater its effect will be, the most effective factorsareareamount of RGO-MWCNT-ZnO/PPynanohybride, followed by immersion time and the number of immersions and pH, respectively. The factors of octanol and quaternary salt dissolution ratio, the amount of nanocomposite inside the hollow fiber, and the scanning speed all indicate that this factor has an insignificant effect on the response which is due to the lower slope of the lines. Thus, the most influential factors are shown in the ANOVA table in the next section.

Figure 3 shows the optimal amount of nanocomposite according to the means of responses for two analytes and indicated that the middle level, *i.e.*, 0.006 g, provided better

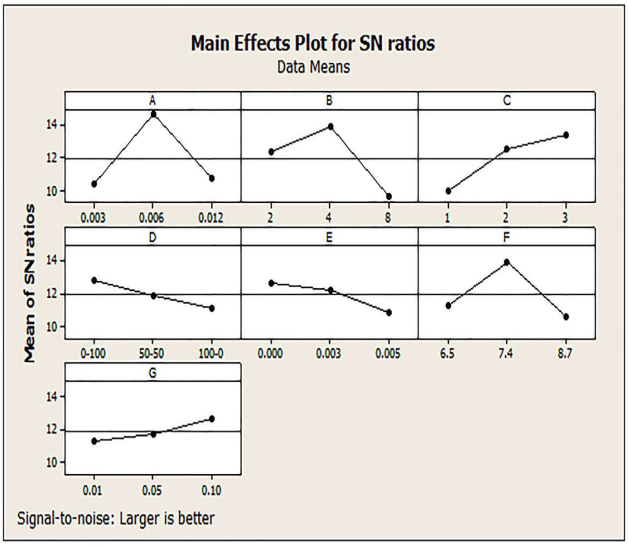

Fig. 3. Results of Taguchi analysis of morphine and Methadone.

results. These results can imply that increasing the number of amounts of nanoparticles to more than 0.006 g, decreases the signal. Because larger amounts of nanocomposite cause instability of the electrode coating surface.

Increasing the immersion time during the coating stage and the number of immersions can affect the uniformity of the coating and later increase the cracks on the surface of the electrode coating during the drying process. On the other hand, a lower number of immersions produces a thinner coating, and thin coatings typically demonstrate porosity. The surface porosity was significantly reduced by increasing the number of layers in multilayer coatings. Thus, the optimal duration of immersion is 4 h, and the number of immersions is 3 times.

The effect of pH as an important variable on the response of the electrode in the simultaneous determination of morphine and methadone was evaluated. On pH values over 8, a slightly decreasing strength of the peak current was noticed. That confirmed that the proton participates in the electrochemical reaction of morphine and methadone oxidation and is also obtained by the dependence of the oxidation potential of the peaks in relation to pH. Moreover, we achieved a greater oxidation peak current at a pH of 7.4 in comparison to other pH values. As a result, the supporting buffer solution pH 7.4 was selected as the optimal value.

Therefore, the supporting buffer solution pH 7.4 was selected as the optimal value. Meanwhile, it is noteworthy that the scan rate influences the oxidation peak current of drugs. This dependency is discussed in detail in the following sections.

Statistical analysis of variance. Table 1 shows the sum of the squares of the main and secondary effects and the total variance and P values. In this table, any factor with the lowest P value is mentioned as the most influential factor. Based on these results, the P values for the main effects of RGO-MWCNT-ZnO/PPy nanocomposite amount were the most effective, while scanning speed was the least effective factor. As the scanning speed has the highest P value, meaning it has the least effect on the electrochemical process of measuring methadone and morphine, where Ssd is the sum of deviations for each factor, and the degree of freedom is equal to the number of measurements-1.

Fisher's test is a statistical tool for checking design parameters that have a significant effect on quality. Herein, F is equal to the ratio of the average square error to the residual error, which is used to identify the significance of a factor. Therefore, the amount of nanocomposite RGO-MWCNT-ZnO/PPy with 83.89% is the most effective factor and the scanning speed with 1.47% is the least effective factor.

INVESTIGATING THE ELECTROCHEMICAL PERFORMANCE OF THE SENSOR

Determining the Active Surface Area of the Electrode

In order to check the performance of the electrode, a simple and effective cyclic voltammetry technique was used. In the cyclic voltammetry method, a 1 mM $[Fe(CN)6]^{3-}/[Fe(CN)6]^{4-}$ a solution containing 0.1 molar potassium chloride was used as a tracer. Figure S6 shows a typical comparison of the cyclic voltammograms of the bare PGE electrode, the sensitized sensor with RGO-MWCNT-ZnO/PPy nanocomposite, and the modified electrode with hollow fiber nanocomposite (RGO-MWCNT-ZnO/PPy-PEG-HF).

Compared to bare PGE, the peak current of modified PGE nanocomposites is an amplified current that shows lower peak separation (ΔE_p). Besides, in the cyclic voltammograms of the modified electrode with hollow fiber nanocomposite (RGO-MWCNT-ZnO/PPy-PEG-HF, compared to the RGO-MWCNT-ZnO/PPy nanocomposite, the observed current also increases and the peak separation shows a greater decrease than the RGO-MWCNT-ZnO/PPy nanocomposite, furthermore, the surface area of the electrode, the number of active points on the electrode and the speed of electron transfer also show an increase. The active surface area of the electrodes has been calculated using Randles-Sevcik Eq. (2):

$$Ipa = (2.69 \times 10\ 5)\ n\ 3/2\ A_0\ D_0 1/2\ C_0 v\ ½ \quad (2)$$

where Ipa is the anode peak current, n is the number of transferred electrons, A_0 is the electrode surface, D_0 is the diffusion coefficient, v is the scan speed and C_0 is the concentration of the probe molecule. Solution of potassium ferrocyanide (1 mM), in the electrolyte of potassium chloride (0.1 M), n is equal to one and D is equal to 7.6×10^{-6} cm^2 s^{-1}. Therefore, by measuring the anodic current of the solution at

Table 1. ANOVA Table for Taguchi Approach

Source	d_f[a]	Ssd[b]	MS[C]	Adj MS	F-Value	F-Value
A	2	39.940	39.940	19.970	9.24	0.004
B	2	29.876	29.876	14.938	6.91	0.010
C	2	22.000	22.000	11.000	5.09	0.025
D	2	9.476	9.476	4.738	2.19	0.154
E	2	7.491	7.491	3.745	1.73	0.218
F	2	21.850	21.850	10.925	5.06	0.026
G	2	4.336	4.336	2.168	1.00	0.395
Residual error	12	25.923	25.923	2.160		
Total	26	160.892				

S = 1.450, R-Sq = 83.89%, R-Sq(adj) = 65.09%. [a]Degree of freedom; [b]Sum of squares; [C]Mean Squares.

different scan speeds ranging from 25 to 200 mV s^{-1} and plotting the anodic current as the square root of the scan rate, a line is obtained and the slope of which shows the effective surface of the electrode.

The effective surface of the bare graphite electrode is 0.125 cm^2, the surface of the electrode modified with RGO-MWCNT-ZnO/PPy nanocomposite is 0.405 cm^2, and the surface of the electrode modified with nanocomposite with hollow fiber (RGO-MWCNT-ZnO/PPy-PEG-HF) is 0.602 cm^2. These results show that the presence of nanocomposite with hollow fiber (RGO-MWCNT-ZnO/PPy-PEG-HF) on the surface of the pen can accelerate the charge transfer process and the number of active sites on the surface of the electrode increases.

Electrochemical Behavior of Manufactured Electrodes

The electrochemical behavior of morphine and methadone on bare electrodes, modified with nanocomposite and with hollow fiber (RGO-MWCNT-ZnO/PPy-PEG-HF) supported nanocomposite, was investigated using differential pulse voltammetry (S7A) and cyclic voltammetry techniques (Fig. S7B) in optimal conditions of phosphate buffer saline (pH 7) at a scanning speed 0.1 V s^{-1} and in the potential range of 0 to 1.2 V.

The voltammogram results of morphine and methadone in a 2 μM solution show that two irreversible oxidation peaks appeared at 0.81 V for methadone and 0.41 V for morphine. The use of sensitized nanocomposite electrode (RGO-MWCNT-ZnO/PPy) with hollow fiber to modify the electrode surface due to the catalytic effect of multi-walled carbon nanotubes and graphene oxide and the unique properties of zinc oxide nanorods, as well as the use of solid/liquid phase microextraction method based on the fiber, causes an increase in the effective surface of the electrode and the charge transfer ability. This produced a significant strengthening of the peak current and the potential of the peaks shifted to lower values, which shows the positive effect of the nanocomposite with hollow fiber (RGO-MWCNT). ZnO/PPy-PEG-HF facilitates the oxidation process of morphine and methadone. Therefore, the use of a sensor modified with hollow fiber-supported nanocomposite (RGO-MWCNT-ZnO/PPy-PEG-HF) is suggested for the quantitative analysis of morphine and methadone.

Oxidation Mechanism of Morphine and Methadone

In the case of the sensitized nanocomposite (RGO-MWCNT-ZnO/PPy) electrode supported by hollow fiber, the oxidation process (diffusion or surface absorption) of the species on the modified electrode can be recorded by investigating the potential growth speed.

For this purpose, differential pulse voltammograms were drawn of a 4 μM solution of morphine and methadone at different scanning speeds in the range of 2 to 200 mV s^{-1} in phosphate-buffered saline (Illustrated in Figs. S8A and S9A). According to the Randles-Swick equation, Ip is proportional to $v^{1/2}$ in diffusion-controlled reactions, whereas Ip equals v in the surface adsorption process, The experimental results (Figs. S8B and S9B) show that with an increase in the scanning speed from 2 to 200 mV/sat a constant concentration of morphine and methadone, the peak potential shifted to more positive peaks and the peak current was continuously on the rise. There is a linear relationship existing between the current intensity and the square root of the scan rate in the morphine and methadone potentials with correlation coefficients R2 = 0.9986 (Eq. (3)) and R2 = 0.9989 (Eq. (4)) respectively, which indicates that the oxidation process of the species was under the diffusion process. Thus, the diffusion-controlled redox reactions of morphine and methadone occurred

$$Y = 12.961X + 0.7654 \quad (3)$$

$$Y = 23.634X + 2.6317 \quad (4)$$

Furthermore, when the logarithms of current peak (logIp) and scan speed (logv) for morphine and methadone (Figs. S8C and S9C) were drawn, a straight line formed – for morphine (Eq. (5)) with a correlation coefficient R^2 = 0.9946 and for methadone (Eq. (6)) with a correlation coefficient of R^2 = 0.9983.

$$Y = 0.3156X + 0.379 \quad (5)$$

$$Y = 0.3378X + 0.0106 \quad (6)$$

The slopes for morphine and methadone were calculated as 0.3378 and 0.3156 v, respectively. These slope values are close to the theoretical value (of 0.5 v) for diffusion-

controlled irreversible reactions, and the yalsoconfirm that the oxidation process of these two drugs is under the control of the diffusion phenomena.

On the other hand, according to Laviron's equation, for the irreversible anodic reactions that are controlled by the diffusion process, the peak potential (E_P) was obtained according to Eq. (7).

$$Epa = E_0 - (RT/(1-\alpha)\, nF)\, \ln((1-\alpha)\, nF/RTKs) + (RT/(1-\alpha)\, nF)\, \ln v \quad (7)$$

In Eq. (7), E_0 is the standard formal potential, α is the electron transfer coefficient, F is the Faraday number (96493 C mol^{-1}), R is the molar constant of perfect gases (314.8 J mol^{-1} K^{-1}), T is the ambient temperature in Kelvin (298 K), and Ks is the transfer rate constant.

There is a linear relationship between the oxidation peak potential (Ep) of morphine and methadone and the logarithm of the scan rate (Figs. S8D and S9D). The number of transferred electrons during the oxidation process can be calculated (n) by taking into account the slope of the Ep curve in terms of logv of morphine and methadone and the logarithm of the scan rate.

The number of exchanged electrons (n) in this process for morphine and methadone is 1.74 (approximately equal to 2) and 2.08 (approximately equal to 2), respectively, which is consistent with the results obtained for the oxidation mechanism of morphine and methadone.

Effect of pH

Another important factor that affects the performance of the presented electrochemical sensors is pH. The electrochemical behavior of morphine and methadone with the hollow fiber-supported nanocomposite modified sensor (RGO-MWCNT-ZnO/PPy-PEG-HF)ina4-micromolar solution of both drugs was scrutinized using the differential-pulse voltammetry method. It showed a pH change in the range of 2 to 10. About morphine, as the pH increased from 4 to 6, the current increased but after pH 6, with any increase in the pH, the peak current decreased, and the highest peak current was observed at pH = 6. In methadone, the peak current rose as the pH increased from 2 to 8, the current fell with arise in pH after that point, and the highest peak current was recorded at pH = 8. (Fig. S10) As a result, on average, for the simultaneous measurement of the two drugs, a pH of 7 was considered to be the optimal pH.

In Figs. S11A and S12A, the peak oxidation potentials for both drugs, morphine, and methadone, in phosphate-buffered saline solution with scanning speed vs-1.1 shifted to more negative potentials with an increasing pH, which shows that protons are also involved in the oxidation process of morphine and methadone.

By plotting the oxidation peak potential (E_{pa}) against the pH for morphine and methadone, a linear relationship was obtained, and this relationship was calculated for morphine with a correlation coefficient of R2 = 0.9984 (in Eq. (8)).

$$E_P = 0.0587 - 0.8187pH \quad (8)$$

The linear relationship of methadone was calculated with the correlation coefficient R = 0.9995 (Eq. (9)).

$$E_P = 0.0579pH + 1.1748 \quad (9)$$

The resulting slopes of these equations (Figs. S13B and S12B) are 0.577 V and 0.585 V for morphine and methadone, respectively, which corresponds almost to the ideal value of 59 mV, illustrating that the number of electrons and protons are the same in the oxidation process of morphine and methadone. The mechanisms of morphine and methadone oxidation are proposed in Fig. 4.

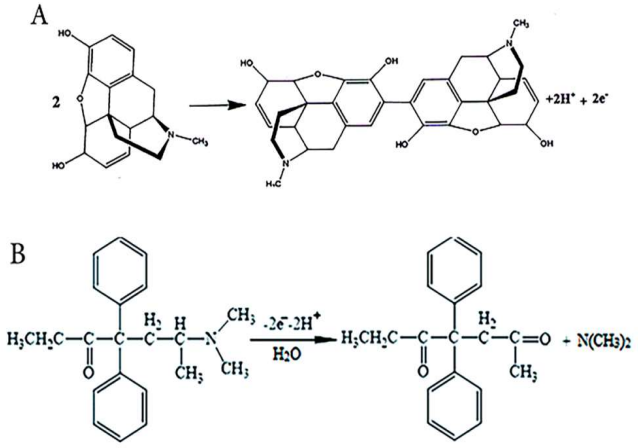

Fig. 4. proposed mechanism of the electrochemical oxidation of (A) morphine (B Methadone.

The proposed mechanism for morphine, as in Fig. AS14, includes the transfer of two protons and two electrons that occurs in this process of oxidation of the third aliphatic amine group in morphine and produces normorphine as a product (Abraham *et al*., 2020). Moreover, the proposed mechanism for methadone (Fig. B4) includes the transfer of two electrons and two protons (Abraham *et al.,* 2020).

Considering the importance of carrier electrolytes in electrochemical reactions, in addition to saline phosphate buffer, different carrier electrolytes such as Robinson's buffer solution and acetate and phosphate buffer were selected for the study. This investigation was conducted in order to determine the best carrier electrolyte for measuring the intensity of the oxidation current of two drugs. The results show that the decomposition signal of morphine and methadone oxidation in phosphate-buffered saline liquid was more and with higher repeatability than in the acetate buffer and phosphate buffer on the surface of this electrode. Therefore, in the following studies, phosphate buffer saline (pH = 7) was used to measure the oxidation of morphine and methadone on the surface of the designed electrode.

Determining the Electron Transfer and Diffusion Coefficient

The Tafel curve was used to determine the electron transfer coefficient. To this end, the data related to the linear sweep voltammograms in the ranges where the kinetics controls the process (the rising part of the diagram) were used (Figs. S13A, S14A)

Using equation 10, the value of α is calculated.

$$LogI = n(1-\alpha)F/2.303RT \quad (10)$$

The TOEFL figure for a concentration of 10 μM with a scan rate of 0.1 V s^{-1} is shown (Figs. S13B, S14B).

The Tafel curve was 1.58 for morphine and 1.63 for methadone, which shows that the determining step of the electrocatalytic process is the charge transfer process of two electrons.

According to the observed slope and TOEFL equation, the value of the transfer coefficient for methadone and morphine was 0.814 and 0.864, respectively.

The chronoamperometry method was used to determine the diffusion coefficient of the studied compounds. The chronoamperograms of the electrode modified with nanocomposite (RGO-MWCNT-ZnO/PPy supported by hollow fiber) were taken. The chronoamperograms of methadone and morphine were with concentrations of 1, 2, and 3 μM, respectively (Figs. 5A and 6A).

The current intensity diagram was drawn in terms of $t^{-1/2}$ for each of the chronoamperograms (Figs. 5A and 6A). Changes in the slope of the graphs I - $t^{-1/2}$ were drawn based on the concentration of morphine and methadone (Figs. 5C, 6C). The number of electrons was equal to two (n = 2), and the diffusion coefficients for morphine and methadone were 1.19×10^{-6} cm s^{-1} and 5.10×10^{-6} cm s^{-1}, respectively.

Investigating the Performance of the Prepared Sensor

Under optimal experimental conditions, the performance of the electrode sensitized with nanocomposite (RGO-MWCNT-ZnO/PPy) with hollow fiber was carried out with the help of simultaneous measurement of standard solutions of morphine and methadone through the differential pulse voltammetry method. To simultaneously characterize the analytes in optimal conditions, DPV was performed at pH = 7, wherein only the concentration of one target molecule was changed and that of the other was kept constant. The peak current of morphine oxidation increased linearly with the increase of its concentration in the range of 0.04 to 100 μM while the peak oxidation current of methadone remained unchanged, at a concentration of 2 μM (Fig. 7A). Similarly, methadone was found in the concentration range from 0.06 to 100 μM in solutions containing morphine with a fixed concentration of 2 μM (Fig. S15A). The simultaneous determination of methadone and morphine was also investigated using the electrode sensitizedwithnanocomposite (RGO-MWCNT-ZnO/PPy) with hollow fiber through the DPV method. Figure S16(A) shows the voltammograms of morphine in various concentrations, indicating that the modified electrode can simultaneously measure morphine and methadone in a wide range of concentrations of each drug thus having an ultra-sensitive determination power. As stated above, a suitable linear relationship exists between the peak oxidation currents of morphine and methadone and their concentrations. In morphine, there are two linear ranges from 1×10^{-5} to 1×10^{-4} and 1×10^{-5} to 4×10^{-8} (Fig. 7B). About methadone, there

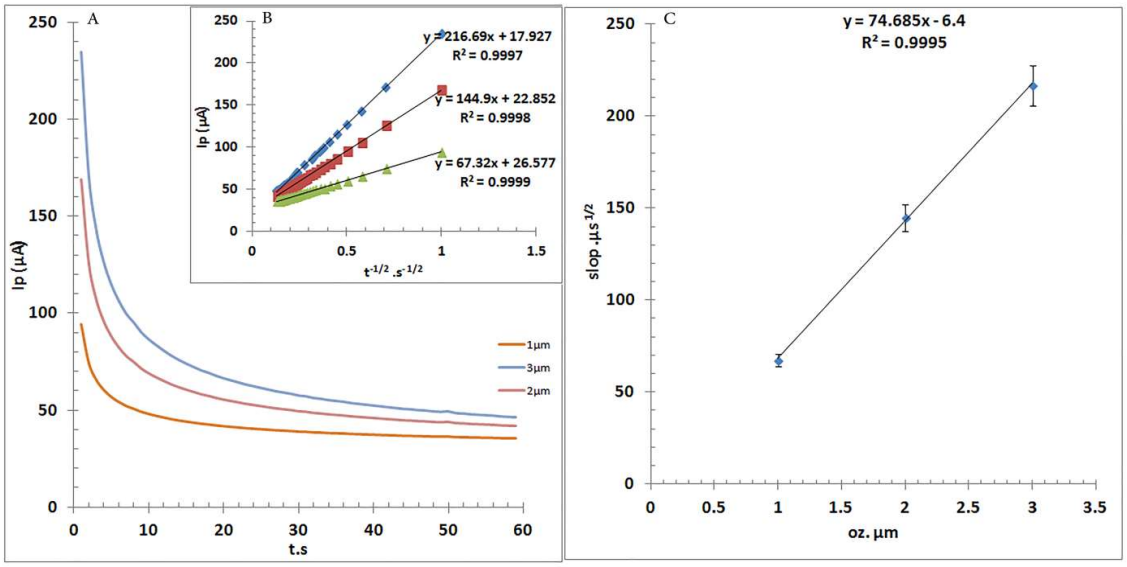

Fig. 5. (A). Chronoamperometric responses of RGO-MWCNT-ZnO-pp coated PGE at a potential step of 800 mV in at the presence of 0.1 molar phosphate saline buffer (pH 7) in the presence of 1-, 2-, and 3-mM morphine. (B) Inset A shows the related plot of I *vs*. $t^{-1/2}$ (C) shows the slopes of the resulting straight lines *versus* the morphine concentration.

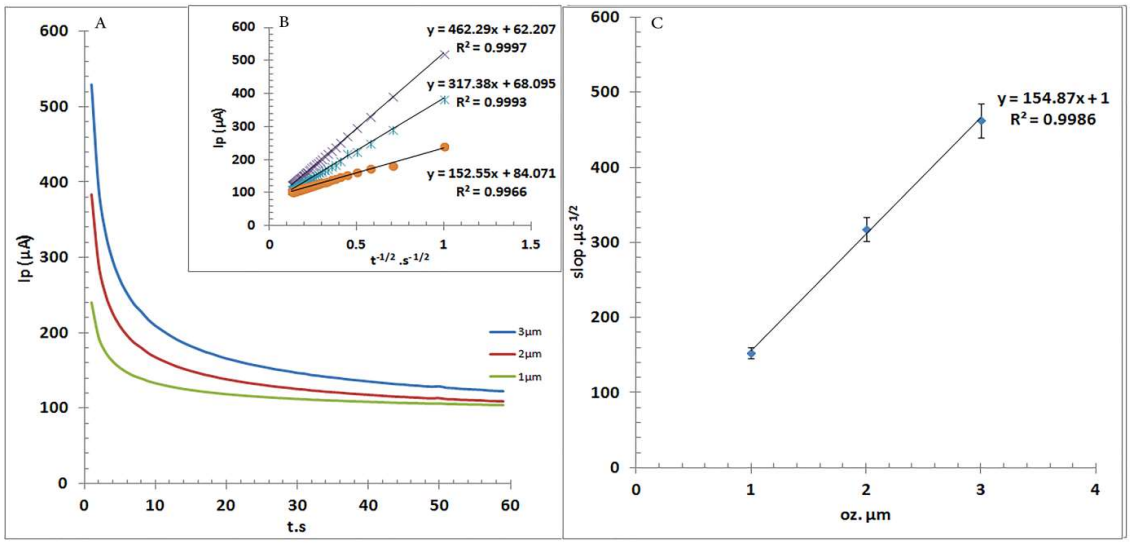

Fig. 6. (A). Chronoamperometric responses of RGO-MWCNT-ZnO- pp coated PGE at a potential step of 500 mV in at the presence of 0.1 molar phosphate saline buffer (pH = 7).in the presence of 1, 2, and 3 mM Methadone. (B) Inset A shows the related plot of I *vs*. $t^{-1/2}$. (C) Shows the slopes of the resulting straight lines *versus* the Methadone concentration.

are two linear ranges, from 1×10^{-4} to 8×10^{-6} and from 8×10^{-6} to 6×10^{-8} (Fig. 15SB).

To evaluate the practical application of the nanosensor, the figures of merit such as the correlation coefficient (R2), the relevant regression equation (slope of the calibration curve indicating the sensitivity), the limit of detection (LOD), and the linear dynamic range (LDR) were investigated under optimal conditions (Table 2).

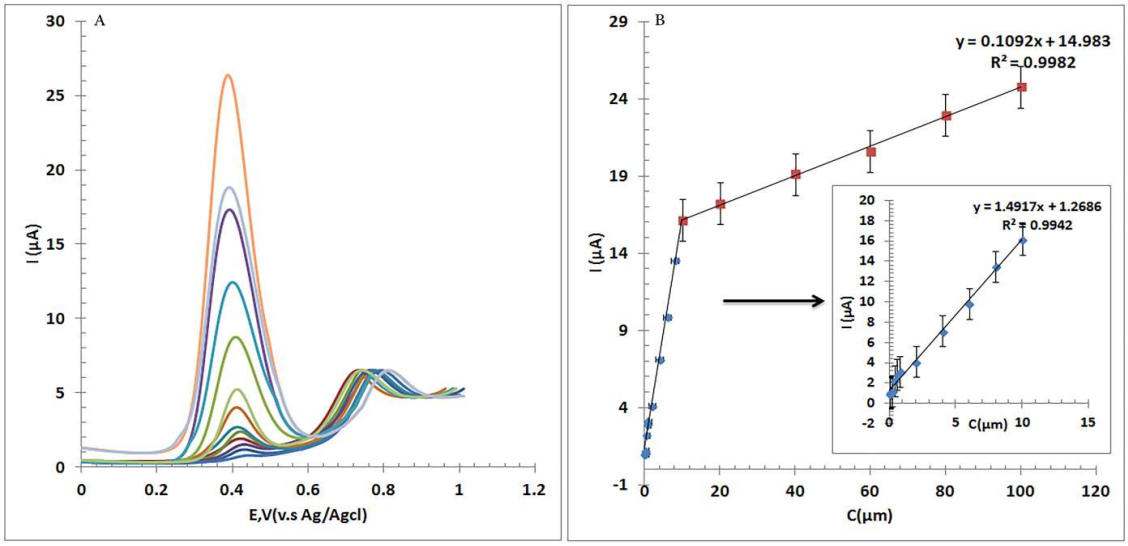

Fig. 7. DP voltammogram obtained from the measurement of morphine with a RGO-MWCNT-ZnO-pp PGE in the presence of phosphate salinebuffer (pH = 7) and scan rate of 0.1 mV s^{-1} at concentrations: 0.04, 0.06, 0.08, 0.8, 1, 2, 4, 6, 8,20, 40,100.

Table 2. Statistical Results of Morphine and Methadone Studies

Statistical calculations	Morphine	Methadone
LDR_a (µM)	0.04-10	0.06-8
	10-100	8-100
Calibration equation (µM)	y = 1.49x + 1.26	y = 1.834x + 1.215
	y = 0.109x + 14.938	y = 0. 331x + 12.325
R^2_b	0.994	0.996
	0.998	0.991
F Test	0.0385	2.8324E-07
T Test	0.014	0.017
LODc	0.012	0.018
RSDd% (n = 3)	2.17	1.28

[a]Linear dynamic range. [b]Correlation coefficient. [c]limits of detection. [d]Relative standard deviation.

The equations of calibration curves were formulated for morphine with two linear ranges namely y (= 1.49x + 1.26) with correlation coefficient R^2 = 0.994and y (= 0.109x + 14.94) with correlation coefficient R^2 = 0.998, and for methadone, the two linear ranges were (= 1.83x + 1.22) with the correlation coefficient R^2 = 0.996 and y (= 0.331x + 12.32) with the correlation coefficient R^2 = 0.991.

The limit of detection (Eq. (11)) is an important analytical factor for evaluating analyte measurements in a given method compared to other methods. A practical approximation for the limit of detection accepted by the Committee on Analytical Chemistry is the concentration of the analyte that has a response equal to the mean response of the blank (yb) plus 3 times the standard deviation of the control sample (Sb).

$$LOD = yb + 3Sb \quad (11)$$

wherein, Sb represents the standard deviation of the blank solution.

In this research, the detection limit of the method for morphine and methadone was 0.0124 and 0.0181 micromolar, respectively. The reproducibility of the method was evaluated by performing 6 repeated measurements on the electrode sensitized with nanocomposite (RGO-MWCNT-ZnO/PPy) supported with hollowfiber in 10 µM morphine and methadone solution. In addition, the value of the standard deviation (RSD) for the measurement of morphine and methadone was obtained at 1.17 and 2.18 respectively.

Figure S16(A) shows the arrangement of the nanocomposite sensor (RGO-MWCNT-ZnO/PPy supported by hollow fiber for the simultaneous measurement of the two drugs, morphine, and methadone, while the concentration of both drugs is constantly changing. It is observed that the modified electrode has a considerable potential to simultaneously measure morphine and methadone in a wide concentration range of both drugs. The equations for the calibration curves have been obtained for morphine in the linear range $y = 0.091x + 0.73$ with the correlation coefficient $R^2 = 0.996$, and for methadone in the linear range of $y = 0.147x + 2.55$ with a correlation coefficient of $R^2 = 0.997$(S16B).

To evaluate the reproducibility of the sensor, the response of the sensor in a 10 µM solution of morphine and methadone using two separate electrodes prepared in similar conditions was investigated. The relative standard deviation was 1.32 and 2.37 for morphine and. 2.62 and 2.08 for methadone. To evaluate the stability of the prepared sensor, the electrode was kept at room temperature for 30 days, after which it showed no significant change (more than 5%) in the response of the electrode to both drugs, indicating the appropriate stability of the sensor. Some analytical characteristics of our electrode were compared with other electrodes made so far to measure morphine and methadone, as shown in Table 3.

The nanocomposite sensor (RGO-MWCNT-ZnO/PPy) supported with hollow fiber has a wide linear range and a lower detection limit compared to other fabricated electrodes.

Investigation of Interference

In order to evaluate the efficiency of the synthesized electrode, the interference effect of different types of interference was evaluated and investigated. The solubility of this electrode in one micromolar concentration of morphine and methadone at pH = 7 was measured by adding 10 times and more concentrations of some interfering species using a voltammetric method.

The interference limit was considered at the concentration at which the interfering species caused a change in the analyte signal of more than 5% of the initial value. If the changes in current are not more than 5%, the presence of that substance can be considered as without interference (Table 4).

The presence of nicotine, fentanyl, naproxen, tramadol, caffeine, and diazepam with a concentration 300 times more and naproxen with a concentration 10 times higher than morphine did not cause a significant change in the drug response.

Regarding methadone, naproxen with a concentration 200 times higher than methadone, tramadol, and fentanyl with a concentration 50 times more than methadone, caffeine, and nicotine with a concentration 100 times higher than methadone, diazepam with a concentration 500 times higher than methadone (µM) is not considered a significant interference in the voltammetric measurement of methadone. Therefore, the present research proved that the prepared nanoparticles can be successfully used to measure morphine and methadone in the presence of other important interfering compounds in aqueous samples.

Application of electrochemical sensor to analyze real samples. In order to evaluate the effectiveness of the proposed method for the simultaneous measurement of morphine and methadone, the designed sensor was used in biological samples of urine and blood. Two samples of urine and blood were spiked with different concentrations of morphine and methadone after initial preparation, then solutions with different concentrations were prepared for (0.2, 0.3, 0.6, 0.9, and 1.2 µM) morphine and (0.2, 0.4, 0.6, 0.8 and 1 µM) methadone. Analytical measurements were carried out using the standard increase method, the results of which are listed in Table 5. The percentage of relative recovery in the range of 98.8-100.22 for morphine and in the range of 98.14-100.58 for methadone shows the high accuracy and applicability of the presented sensor for the simultaneous measurement of small amounts of morphine and methadone in pharmaceutical and biological samples.

Table 3. An Analytical Comparison of the Current Method and some Previous Techniques on the Determination of Morphine and Methadone

Working electrode	Method	Linear range Morphine (μM)	LOD Morphine (μM)	Recovery Morphine	Linear range Methadone (μM)	LOD Methadone (μM)	Recovery methadone	Ref.
M-CNF/CPE[a]	CV-DPV	0.003-55 55-245	0.0019	98-105	-	-	-	[37]
RhN-MC-modified GCE[b]	DPV	0.1-20	0.004	98.2-103.4	-	-		[38]
gold nanoparticles (AuNPs) and polythiophene (p(Thp)) thin film	CV-DPV	-	-	-	0.049-9.9 9.9-29	0.014	98.45-100.60	[39]
(PDDA)/MWCNT/CQD[c]	DPV	-	-	-	0.1-225	0.03		[40]
β-MnO_2 nanoflowers	DPV	0.1-200.0	0.056	98- 103.3	0.1-250.0	0.082	97.3-102	[41]
RGO-MWCNT-ZnO-pp	CV-DPV	. 0.04-10 10-100	0.012		0.06-8 8-100	0.081	98.14-100.5	This work

[a]M-CNF, magnetic carbon nanofiber CPE, carbon paste electrode. [b]RhN, rhodium nanoparticle; MC, mesoporous carbon; GCE. [c]Poly (diallyldimethylammonium chloride) (PDDA)/MWCNT/carbon quantum dots (CQDs).

Table 4. Investigating the Selectivity Effect

Drugs	Structure	Tolerance limit (morphine)	RSD% morphine (n = 3)	Tolerance limit (Metadone)	RSD% Metadone (n = 3)
Nicotine	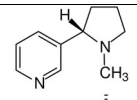	300	3.85	100	4.45
Naproxen	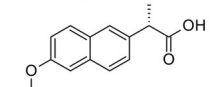	10	4.32	200	4.18
Fentanyel	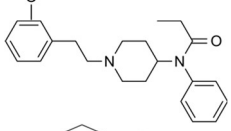	300	3.87	50	4.10
Tramadol	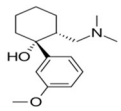	300	3.89	50	4.05
Coffeine	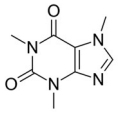	500	3.52	100	4.61
Diazepam	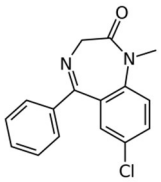	300	3.90	500	4.11

*The tolerance limit is the maximum concentration of interferent which causes an error less than ± 5%.

Table 5. Analytical Results for Simultaneous Determination of Methadone and Morphine in Serum Samples

	Added (μM)		Found ± δ (μM)		RSD%[a] (μM)		RR%[b]	
Sample	Metadone	Morphine	Metadone	Morphine	Metadone	Morphine	Metadone	Morphine
Sample # 1	0	0	0	0	0	0	0	0
Blood serum	0.3	0.3	0.297 ± 0.012	0.301 ± 0.002	3.89	0.84	98.89	100.22
	0.6	0.6	0.598 ± 0.0106	0.594 ± 0.0093	1.77	1.56	99.6	99.06
	0.9	0.9	0.900 ± 0.0092	0.900 ± 0.0190	1.02	2.1	100	100
	1.2	1.2	1.201 ± 0.029	1.207 ± 0.0201	2.39	1.66	100.55	100.58
	0	0	0	0	0	0	0	0
Sample # 2 Blood serum	0.3	0.3	0.298 ± 0.007	0.299 ± 0.004	2.28	1.206	99.2	99.66
	0.6	0.6	0.596 ± 0.022	0.602 ± 0.005	3.78	0.82	99.33	100.27
	0.9	0.9	0.9 ± 0.015	0.883 ± 0.029	1.68	3.26	100	98.14
	1.2	1.2	1.203 ± 0.024	1.196 ± 0.012	1.96	1.04	100.22	99.6
	0	0	0	0	0	0	0	0
Sample # 1 Urine	0.2	0.2	0.197 ± 0.003	0.197 ± 0.003	1.55	1.55	98.33	99.33
	0.4	0.4	0.398 ± 0.005	0.398 ± 0.006	1.16	1.47	99.4	99.4
	0.6	0.6	0.611 ± 0.024	0.607 ± 0.015	3.9	2.49	101.77	101.22
	0.8	0.8	0.804 ± 0.026	0.809 ± 0.030	3.19	3.7	100.54	101.08
	0	0	0	0	0	0	0	0
Sample # 2 Urine	0.2	0.2	0.198 ± 0.007	0.205 ± 0.006	3.64	2.82	99	102.33
	0.4	0.4	0.399 ± 0.010	0.395 ± 0.009	2.57	2.41	99.67	98.75
	0.6	0.6	0.607 ± 0.01	0.607 ± 0.015	1.64	2.51	101.22	101.11
	0.8	0.8	0.793 ± 0.021	0.795 ± 0.008	2.62	1.017	99.16	99.33

RR%: Relative Recovery%.

CONCLUSIONS

This study confirmed the possibility of making a new type of electrochemical biosensor with rGO-MWCNT-ZnO/PPy nanohybrid supported with hollow fiber for the simultaneous determination of methadone and morphine. The fiber was decorated with nanoparticles and quaternary salts, and then the differential pulse voltammetry method was used to measure small amounts of morphine and methadone. The use of quaternary azo salts as a selective agent used in hollow fiber cavities led to appropriate concentrations of morphine and methadone.

Furthermore, the use of nanocomposite (RGO-MWCNT-ZnO/PPy) to modify the surface of the electrode and increase the speed of electron transfer on the surface of the electrode reduced the overvoltage and increased the sensitivity of the method.

As was mentioned before, zinc oxide (ZnO) is an n-type semiconductor with a wide band gap at room temperature (about 3.4 eV), biocompatibility, high electrochemical activities, and non-toxicity. ZnO nano-metal particles have been widely used for the fabrication of electrochemical sensors [42] due to their large surface area, impressive activity, and good stability. ZnO has been synthesized in different morphologies, for example, nanorods, nanowires, nanoparticles, and microspheres, to enhance the surface/volume ratio and photocatalytic activity.

Graphene, with its exclusive structure, contains a 2-dimensional layer of sp2-bonded carbon atoms arranged in a honeycomb lattice. Its significant applications in electrochemical sensors are due to its large surface area, and charge mobility [43].

But, the stacking of graphene sheets is inevitable due to π-π interaction between the end-to-end nanosheets, which reduces the contact surface and charge transfer. It should also be noted that carbon nanotubes are another kind of carbon-based material with a one-dimensional structure and higher performance, Carbon nanotubes (CNTs) are well-known materials for the fabrication of electrochemical sensors too, because of the high surface area, high electrical conductivity, outstanding charge-transport character and high chemical stability which have been used for the preparation of electrochemical sensors in recent years.

These conclusions lead to the fact that the removal efficiency of rGO-CNT-ZnO was much better than each of these sorbents for the removal of the analytes. From now, the combination of ZnO nanoparticles with reduced graphene and CNTs is considered to concept of a three-dimensional network that may enhance the property of composites. The modified electrode was successfully used for the simultaneous determination of methadone and morphine in human urine and blood serum samples.

REFERENCES

[1] V.P. Dole, JAMA 215 (1971) 1131.

[2] P. Abraham, S. Renjini, P. Vijayan, V. Nisha, K. Sreevalsan, V. Anithakumary, J. Electrochem. Soc. 167 (2020) 037559.

[3] P. Alam, S. Borkokoty, M.K. Siddiqi, A. Ehtram, N. Majid, M. Uddin, R.H. Khan, ACS Chem. Neurosci. 10 (2018) 182.

[4] I.B. Anderson, T.E. Kearney, West. J. Emerg. Med. 172 (2000) 43.

[5] N. Wilson, M. Kariisa, P. Seth, H. Smith IV, N.L. Davis, Morb. Mortal. Wkly. Rep. 69 (2020) 290.

[6] M.M. Friciu, H. Alarie, M. Beauchemin, J.M. Forest, G. Leclair, Can. J. Hosp. Pharm. 73 (2020) 141.

[7] K. Allen, R. Azad, H. Field, D. Blake, Ann. Clin. Biochem. 42 (2005) 277.

[8] A. Farahani, H. Sereshti, Anal. Bioanal. Chem. 412 (2020) 129.

[9] M. Khodaei, A. Esmaeili, ACS Biomater. Sci. Eng. 6 (2019) 246.

[10] J.A.M. Pulgarín, L.F.G. Bermejo, J.M.L. Gallego, M. N.S. García, Talanta 74 (2008) 1539.

[11] A.S. Trajanovska, V. Vujovic, L. Ignjatova, D. Janikevik Ivanovska, A. Chibishev, Med. Res. Arch. 67 (2013) 48.

[12] D.J. Christoffersen, C. Brasch-Andersen, J.L. Thomsen, M. Worm-Leonhard, P. Damkier, K. Brøsen, Forensic Science, Clin. Med. Pathol. 11 (2015) 193.

[13] Z. Nazari, Z. Es' haghi, Anal. Bioanal. Electrochem. 14 (2022) 228.

[14] E. Verrinder, N. Wester, E. Leppanen, T. Lilius, E. Kalso, B.R. Mikladal, I. Varjos, J. Koskinen, T. Laurila, ACS Omega 6 (2021) 11563.

[15] S.M. Khoshfetrat, P.S. Dorraji, L. Fotouhi, M. Hosseini, F. Khatami, H.R. Moazami, K. Omidfar, Sens. Actuators B: Chem. 364 (2022) 131895.

[16] S.M. Khoshfetrat, P. Hashemi, A. Afkhami, A. Hajian, H. Bagheri, Sens. Actuators B: Chem. 348 (2021) 130658.

[17] X. Chen, M. Peng, X. Cai, Y. Chen, Z. Jia, Y. Deng, B. Mei, Z. Jiang, D. Xiao, X. Wen, N. Wang, H. Liu, D. Ma, Nat. Commun. 12 (2021) 2664.

[18] M. Derakhshi, S. Daemi, P. Shahini, A. Habibzadeh, E. Mostafavi, A.A. Ashkarran, J. Funct. Biomater. 13 (2022) 27.

[19] A.M.B. F.Soares, C.L.C. Carvalho, G. de Andrade Rodrigues, R.A. Luz, E.T. Gerôncio, W. Cantanhêde, Adv. Biochem. 1 (2022) 89.

[20] M. Hilal, W. Yang, Nano Converg. 9 (2022) 278.

[21] L. Yan, T. Xiong, Z. Zhang, H. Yang, X. Zhang, Y. He, J. Bian, H. Lin, D. Chen, Compos. Part A Appl. Sci. Manuf. 157 (2022) 106913.

[22] K. Harpale, P. Kolhe, P. Bankar, R. Khare, S. Patil, N. Maiti, M. Chaskar, M.A. More, K.M. Sonawane,. Synth. Met. 269 (2020) 116542.

[23] H.G. Ugland, M. Krogh, L. Reubsaet, J. Chromatogr. B 798 (2003) 127.

[24] Z. Es'haghi, A. Nezhadali, S. Bahar, S. Bohlooli, A. Banaei, J. Chromatogr. B 980 (2015) 55.

[25] M. Galiński, A. Lewandowski, I.Stępniak, Electrochim. Acta 51 (2006) 5567.

[26] C.C. Chan, W.C. Hsu, C.C. Chang, C.S. Hsu, Sens. Actuators B: Chem. 145 (2010) 691.

[27] R. Pashley, M. Francis, M. Rzechowicz, Water 35 (2008) 67.

[28] S. Stankovich, D.A. Dikin, G.H. Dommett, K.M. Kohlhaas, E.J. Zimney, E.A. Stach, R.D. Piner, S.T. Nguyen, R.S. Ruoff, Nature 442 (2006) 282.

[29] Y. Li, J. Liu, Y.Zhang, M. Gu, D. Wang, Y.Y. Dang, B. C. Ye, Y. Li, Biosens. Bioelectron. 106 (2018) 71.

[30] J. Xu, Y. Wang, Y. Xian, L. Jin, K. Tanaka, Talanta 60 (2003) 1123.

[31] P. Patil, G. Gaikwad, D. Patil, J. Naik, Phys. Rev. 39 (2016) 777.

[32] S. Yang, C. Shen, X. Lu, H. Tong, J. Zhu, X. Zhang, H.J. Gao, Electrochim. Acta 62 (2012) 242.

[33] C. Mahajan, P. Chaudhari, S. Mishra, J. Mater. Sci. Mater. Electron. 29 (2018) 8039.

[34] S. Sadeghi, A. Motaharian, A.Z. Moghaddam, Sens. Actuators B Chem. 168 (2012) 336.

[35] K.A. Escamilla-Lara, A.C. Heredia, A. Peña-Alvarez, I. S. Ibarra, E. Barrado, J.A. Rodriguez, Molecules 25 (2020) 2924.

[36] X. Zhu, L. Lu, X. Duan, K. Zhang, J. Xu, D. Hu, Y. Wu, J. Electroanal. Chem. 731 (2014) 84.

[37] G. Bahrami, H. Ehzari, S. Mirzabeigy, B. Mohammadi, E. Arkan, Mater. Sci. Eng. C 106 (2020) 110183.

[38] M. Jahanbakhshi, Sens. Actuators B Chem. 97 (2019) 479.

[39]Z. Khorablou, F. Shahdost-Fard, H. Razmi, Sens. Actuators B Chem. 344 (2021) 130284.

[40] B. Rezaei, A. Tajaddodi, A.A. Ensafi, Food Anal. Methods 12 (2020) 5210.

[41] S. Akbari, S. Jahani, M.M. Foroughi, H. Hassani Nadiki, RSC Adv. 10 (2020) 38532.

[42] P. Nayak, B. Anbarasan, S.J. Phys. Chem. 117 (2013) 13202.

[43] M. Kim, Y. Hwang, J. Kim, Chem. Phys. 16 (2014) 351.